Exp Brain Res (2007) 176:227–236
DOI 10.1007/s00221-006-0608-2

RESEARCH ARTICLE

Prostaglandin E_2 potentiates the excitability of small diameter trigeminal root ganglion neurons projecting onto the superficial layer of the cervical dorsal horn in rats

Jun Kadoi · M. Takeda · S. Matsumoto

Received: 3 March 2006 / Accepted: 16 June 2006 / Published online: 19 July 2006

Abstract The aim of the present study was to investigate how prostaglandin E_2 (PGE_2) affects the excitability of trigeminal root ganglion (TRG) neurons, projecting onto the superficial layer of the cervical dorsal horn, using fluorescence retrograde tracing and perforated patch-clamp techniques. TRG neurons were retrogradely labeled with fluorogold (FG). The cell diameter of FG-labeled neurons was small (< 30 μm). Under the voltage-clamp mode, application of PGE_2 (0.01–10 μM) concentration-dependently increased the magnitude of the peak tetrodotoxin-resistant sodium current (TTX-R I_{Na}) and this current was maximal at a concentration of 1 μM. One micromolar PGE_2 application caused a hyperpolarizing shift of 8.3 mV in the activation curve for TTX-R I_{Na}. In the current-clamp mode, the PGE_2 (1 μM) application significantly increased the number of action potentials during the depolarizing step pulses as well as the level of overshoot but had no significant effect on the resting membrane potential. These results suggest that the excitability of small diameter TRG neurons seen after 1 μM PGE_2 application is involved in an increase in the TTX-R I_{Na}.

Keywords Prostaglandin E_2 · Trigeminal root ganglion · Retrograde-labeling C_1 neurons · TTX-resistant Na^+ channel

J. Kadoi (✉) · M. Takeda · S. Matsumoto
Department of Physiology, Nippon Dental University, School of Dentistry at Tokyo, 1-9-20, Fujimi-cho, Chiyoda-ku, Tokyo, 102-8159, Japan
e-mail: j-kadoi@tky.ndu.ac.jp

Introduction

It is well known that nociceptive information from the area innervated by the trigeminal nerve, including tooth pulp (TP), projects onto the trigeminal spinal nucleus oralis (SpVo) and caudalis (SpVc) (Sessle 1987; Dallel et al. 1988). As the histological structures of the first cervical dorsal horn (C_1) have an analogy to the SpVc region, electrophysiological studies reveal that convergent inputs from TP, TMJ and masseter muscle are considered to be terminated in the C_1 segment of the spinal cord (Matsumoto et al. 1999; Tanimoto et al. 2002; Takeda et al 2005; Nishikawa et al. 2004). This is further supported by the anatomical evidence showing that central projections of the TP and masseter muscle afferent fibers onto C_1 neurons were found in rats (Arvidsson and Raappana 1989; Marfurt and Turner 1984). Bereiter et al. (2000) indicated the possibility that the nociceptive inputs from deep craniofacial tissues are relayed to the ventral trigeminal subnucleus interpolaris/caudalis transition region (SpVi/Vc-vl) through the trigeminal subnucleus caudalis/cervical dorsal horn C_2 (SpVc/C_2) junction region. C_1 spinal neurons are known to contribute to the pain referred to the neck and jaw regions because the neurons responding to electrical stimulation of the ipsilateral and contralateral phrenic nerves above the heart are also excited by noxious stimulation of somatic receptive fields involving the neck and jaw regions (Razook et al. 1995). Similarly, Matsumoto et al. (1999) also demonstrated that most of C_1 spinal neurons responding to TP stimulation receive afferent inputs from the ipsilateral phrenic nerve. From these observations, it is therefore possible that there is a convergence of face, neck, jaw, TP and phrenic afferents

on the same C_1 spinal neurons in rats, and that C_1 spinal neurons play an important role in the referred pain associated with dental pain.

Conveying nociceptive information from the peripheral receptive field to the C_1 spinal dorsal horn consists mainly of the small diameter (Aδ/C) fiber types terminating the superficial layers of the C_1 spinal dorsal horn (Light and Perl 1979; Sugiura et al. 1986). Recently, we reported that the activation of μ-opioid receptors inhibited the excitability of small diameter trigeminal root ganglion (TRG) neurons projecting onto the superficial layers of the cervical dorsal horn, using the fluorogold (FG)-retrograde labeling technique (Takeda et al. 2004). Since the recording from the cell body of DRG neurons is a simple and accessible model for studying the characteristics of peripheral and/or central terminals of the axonal membrane (Hu and Li 1996), the recording from the cell body of TRG neurons is assumed to faithfully reflect the characteristics of the peripheral terminals in the trigeminal receptive field.

Peripheral inflammation caused by tissue damage results in pain, reflecting an increase in the excitability of primary afferent neurons innervating their area. It has been reported that many inflammatory mediators, such as prostaglandin E2 (PGE_2), bradykinin and 5-hydroxytryptamine (5-HT), sensitize the excitability of peripheral terminals in the small diameter dorsal root ganglion (DRG) neurons (Dray 1995). There is a report that capsaicin- and PGE_2-sensitive DRG neurons more frequently express TTX-R I_{Na} compared to the case of capsaicin-insensitive neurons (Peace and Duchen 1994; Arbuckle and Docherty 1995). In small diameter DRG and nodose ganglia (NG) neurons, PGE_2 shifts the activation curve of the TTX-R I_{Na} to more negative potentials and enhances the amplitudes of the current (England et al. 1996; Gold et al. 1998; Kwong and Lee 2005; Matsumoto et al. 2005). In one of these studies an intracellular perfusion of the neurons with an inhibitor of protein kinase A (PKA) abolished the excitatory effect of PGE_2 on TTX-R I_{Na} (Matsumoto et al. 2005). These observations were consistent with a report that application of either 5-HT or ATP potentiates TTX-R I_{Na} in the nociceptive DRG neurons (Gold 1999). Taken together, it is possible to speculate the idea that an increase in the TTX-R I_{Na} contributes to the development of the trigeminal hyperalgesia. Thus, the question arises as to whether PGE_2 modulates the excitability of the small diameter TRG neurons, which are able to be identified by the superficial layer of the cervical dorsal horn, via the modulation of TTX-R I_{Na}. Nevertheless, there are no studies examining the effect of PGE_2 on TTX-R I_{Na} in the TRG neurons retrogradely labeled.

The purpose of the present study was to examine whether PGE_2 modulates the excitability of small diameter TRG neurons, projecting onto the superficial layer of the cervical dorsal horn, via the modulation of TTX-R I_{Na}, using retrograde-tracing and perforated-patch techniques.

Materials and methods

The experiments were approved by the Animal Use and Care Committee of Nippon Dental University and were consistent with the ethical guidelines of the International Association for the Study of Pain (Zimmermann 1983). Efforts were made to minimize the number of animals used and their suffering.

Retrograde-labeling of TRG neurons

Seventeen rat pups (P8-P12) were deeply anesthetized with ketamine/xylazine (42 mg/kg and 5 mg/kg, respectively, i.m.), and the dorsal surface of the first cervical spinal cord segments were surgically exposed. Fluorogold (FG; 2%, 0.5 μl; Fluorochrome, Englewood, CO, USA) was injected bilaterally into the dorsal surface of the cervical spinal cord (depth, 100–250 μm) with pressure injection through a glass micropipette attached to a micromanipulator (tip diameter of 30–50 μm; Fig. 1a). After the FG injection, the skin incision was sutured. The pups were allowed to recover and were returned to a lactating mother.

Acute dissociation of TRG neurons

Two to four days after FG injection, dissociation of TRG neurons was conducted as described in a previous study (Takeda et al. 2004). After the decapitation of neonatal rats anesthetized with pentobarbital (50 mg/kg, i.p.), a pair of trigeminal ganglia were dissected and incubated in Ca^{2+}- and Mg^{2+}-free Hank's balanced salt solution (HBSS) (Invitrogen Corp., Carlsbad, CA, USA) containing (in mM) 130 NaCl, 5 KCl, 0.3 KH_2PO_4, 4 $NaHCO_3$, 0.3 Na_2HPO_4, 5.6 glucose and 10 *N*-2-hydroxyethylpiperazine-*N*′-2-ethane-sulfonic acid (HEPES), pH 7.3. They were incubated for 15–25 min at 37°C in HBSS containing 20 unit/ml of papain (Worthington Biochemical, Freehold, NJ, USA). The cells were dissociated by trituration with a fire-polished Pasteur pipette and subsequently were plated onto poly-L-lysine-pretreated 35-mm dishes. The plating medium contained Leibovitz's L-15 solution (Invitrogen Corp.) supplemented with (concentration and millimolar) 10% newborn calf serum, 50 U/ml penicillin–streptomycin

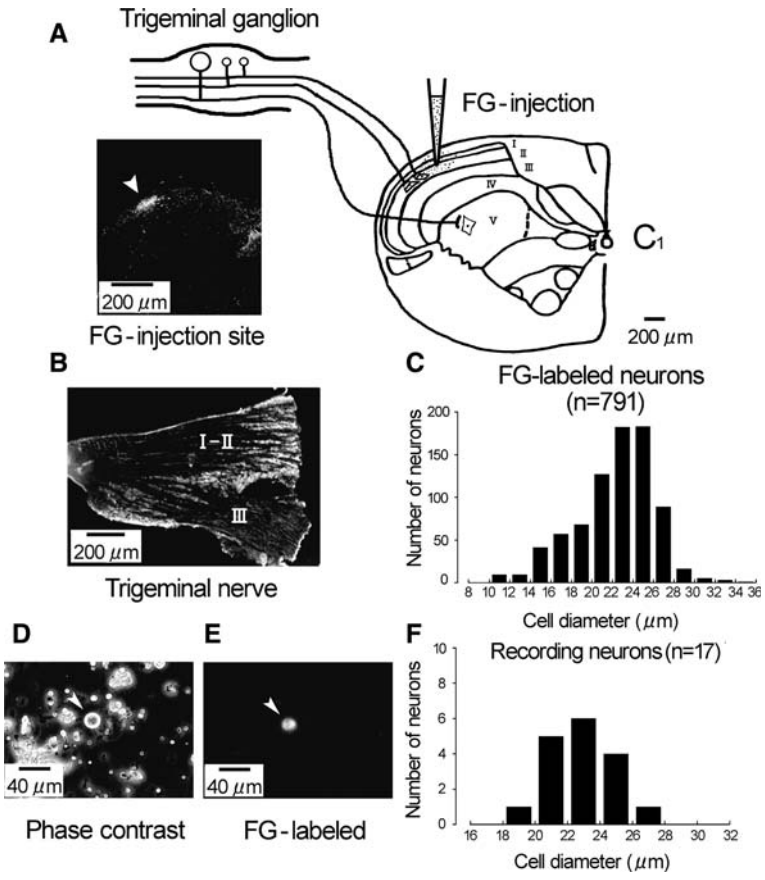

Fig. 1 Retrograde labeling of TRG neurons projecting onto the superficial layer of the cervical dorsal horn. **a** Schematic drawing of method to show a retrograde labeling of TRG neurons with 2% FG (0.5 μl) injection to the superficial layer of the cervical dorsal horn. *Inset* location of 2% FG-injection sites. **b** Light microscopic observation of the trigeminal nerve (I–III). **c** Distribution of cell diameter of FG-labeled TRG neurons. **d, e:** Dissociated TRG neurons (diameter 20 μm) observed under phase contrast optics (**d**), and the C_1 neuron identified by the fluorescent FG in the same field (**e**). **f** Size distribution of dissociated FG-labeled TRG neurons recorded (n = 17)

(Invitrogen Corp.), 26 mM $NaHCO_3$ and 30 mM glucose. The cells were maintained in 5% CO_2 at 37°C. The cells were used for recording between 2 and 8 h after plating.

Recording solution and drugs

The composition of the extracellular recording solution used in these experiments is shown in Table 1. In voltage-clamp experiments, 1 μM tetrodotoxin (TTX) was added to the extracellular solution. Some recordings were performed in the current-clamp mode also, and we used quasiphysiological recording solutions in this study (Table 1). In current-clamp experiments, 1 μM TTX was added to the extracellular solution. All experiments were performed at room temperature (21–26°C). PGE_2 (Sigma-Aldrich, St Louis, MO, USA) was dissolved as a stock solution of 1 mM in distilled water, stored at −20°C and diluted in the external solution before use.

Whole cell-patch clamp recording

FG-labeled TRG neurons were identified by applying a short pulse of UV light (340–380 nm) and by capturing the image of fluorescent cells with a microscope (Nikon, Tokyo, Japan). The locally developed software permitted the superposition of a tracing of the perimeter of the fluorescent cell onto the image of the same cell in the ganglion visualized with visible light. Whole-cell patch recordings were conducted with a rapid perforated-patch clamp technique (Rae et al. 1991; Takeda et al. 2004). The fire-polished patch-pipettes (2–5 MΩ) were filled with an internal solution of amphotericin B (100 μg/ml) and lucifer yellow dipotassium salt (0.1% Sigma) (Table 1). Current- and voltage-clamp recordings were conducted with an Axopatch 200B amplifier (Axon Instr., Foster City, CA, USA). Signals were low-pass filtered at 1 or 5 kHz and digitized at 10 kHz.

Neurons were always bathed in a flowing stream of the external solution except during the application of drugs. After seal formation and membrane perforation, leakage and capacitive transients were cancelled by the analog circuitry. The series resistance compensation (> 80%) was employed. The recording chamber (volume, 0.5 ml) was mounted on an inverted microscope (Nikon) equipped with a phase-contrast video camera. The chamber was perfused under gravity with the external solution at approximately 0.5 ml/min.

Table 1 Composition of extra- and intracellular solution

	V-clamp		*I*-clamp	
Extracellular solutions (mM)	NaCl	60	NaCl	160
	Choline chloride	50	HEPES	10
	TEA	40	KCl	5
	HEPES	10	$CaCl_2$	2
	$MgCl_2$	3	$MgCl_2$	1
	Glucose	10	Glucose	10
	TTX	0.001	TTX	0.001
	Adjusted to pH = 7.4 with TEAOH		Adjusted to pH = 7.3 with NaOH	
Intracellular solutions (mM)	CsF	110	Potassium gluconate	130
	CsCl	40	KCl	20
	HEPES	10	EGTA	10
	NaOH	10	HEPES	10
	EGTA	2	Na_2-Creatine phosphate	5
	$MgCl_2$	2	Mg-ATP	2
			$CaCl_2$	1
			Na-GTP	0.1
	Adjusted to pH = 7.2 with CsOH		Adjusted to pH = 7.2 with KOH	

TEA Tetraethylammonium chloride, *EGTA* ethyleneglycol-bis(β-aminoethyl ether)-*N, N, N′,N′*,-tetra acetic acid

In the voltage-clamp mode, TTX-R I_{Na} was recorded before and after 2 min of PGE_2 (0.01–10 μM) applications. The current–voltage (*I–V*) relationship was first monitored using step pulses (50 ms) from the holding potential of −80 to + 60 mV in 5 mV increments at 5-s intervals.

In the current-clamp mode, we determined the threshold (1T) for action potentials. The threshold was defined as the current value for eliciting a depolarizing single pulse (100–400 pA, 300 ms). The firing rates of action potentials before and after the PGE_2 (1 μM) application were assessed by counting the number of action potentials elicited by depolarizing pulses (1T, 2T and 3T). The resting membrane potential, spike duration and height of overshoot were also assessed before and after PGE_2 applications. Spike duration was determined as the duration of the first spike at the level of half-amplitude.

Data analysis

Digital images were collected and stored on a laboratory computer and later analyzed by means of Adobe Photoshop 7.0 and Cannvas. Data acquisition and analysis were performed with p-clamp 8.0 (Axon Instrument). Steady-state activation curves were fitted by using the Boltzmann function, $G/G\max = 1/[1 + \exp(V_{1/2} - V_m)/k]$, where V_m is the prepulse membrane potential, $V_{1/2}$ is the membrane potential at which 50% activation of the voltage is observed and k is the slope factor. Data are expressed as means ± standard error of the mean (SEM). Statistical analysis (Student's *t* test for paired samples) was performed using Excel 2000 software and $P < 0.05$ was considered statistically significant.

Histological confirmation for C_1 dorsal horn and retrograde-labeling of TRG neurons

FG-injected rats ($n = 8$) were anesthetized with pentobarbital sodium (50 mg/kg i.p.), and transcardially perfused with 50 ml heparinized saline in 0.01 M phosphate-buffered saline (PBS) followed by 100 ml of 4% paraformaldehyde in 0.1 M phosphate-buffer (pH 7.3). The TRGs and cervical dorsal horn were removed and incubated in 10 and 20% sucrose solution (1 h each) and 30% overnight.

Frozen tissue was sectioned at 22 μm with a cryostat (Leica, Germany) and mounted on silane-coated glass slides. Using fluorescence microscope, we identified the deposits of FG in the superficial layer of C_1 spinal dorsal horn, measured the cell diameter of FG-labeled neurons and calculated their numbers.

Results

Retrograde-labeling of TRG neurons onto the superficial layer of the cervical dorsal horn

Figure 1a shows a schematic drawing of the retrograde-labeling of a TRG neuron after FG injection, which was located onto the superficial layer of the cervical dorsal horn. There were many FG deposits in the

superficial layer in the C_1 dorsal horn (Fig. 1a lower left panel). The areas innervated by the three branches of the trigeminal nerve are retrogradely labeled (Fig. 1b). Figure 1c shows the distribution of FG-labeled TRG neurons. Of the 791 FG-labeled TRG neurons, 597 (75.5%) were within 20–30 μm (cell diameter). Figure 1d shows a typical example of dissociated FG-labeled TRG neurons under the phase contrast optic, and the identified same C_1 neuron was confirmed by the appearance of a fluorescent FG in the same field (Fig. 1e). As shown in Fig. 1f, most of the FG-labeled TRG neurons recorded were small-sized neurons.

Time-dependent effects of internal fluoride on the TTX-R Na^+ current

In this study, we used FG-labeled TRG neurons (soma diameter; 22.1 ± 0.4 μm, $n = 17$). In acutely dissociated TRG neurons after perforation of the cell membrane with amphotericin B, series resistance dropped to below 20 MΩ (14.7 ± 0.7 MΩ, $n = 17$) within 5–10 min and remained stable (10–20 MΩ) for over 15 min. The mean values for cell capacitance were 17.9 ± 1.1 pF ($n = 17$). The peak amplitudes of TTX-R I_{Na} in the six labeled and unlabelled TRG neurons were −2.6 ± 0.4 and −2.9 ± 0.2 nA, respectively, but their values did not show any statistical significant difference. To determine whether fluoride (F^-) contained in the internal solution induces the change in the peak TTX-R I_{Na} as well as in the activation curve, we examined the time-dependent effects of F^- on TTX-R I_{Na} properties. After obtaining the whole-cell mode (series resistance dropped to below 20 MΩ), a rapid increase in the TTX-R I_{Na} occurred, and 5 min after 1 μM TTX application the amplitude of the current was stabilized. As shown in Fig. 2a, b, no significant changes in TTX-R I_{Na} evoked by depolarizing pulses (−80 to + 60 mV) were found at 5 min intervals for 15 min. Figure 2c, d shows the time-course effects of internal F^- on the TTX-R I_{Na} in five cells. The peak amplitude of TTX-R I_{Na} did not change significantly (Fig. 2b, c).

Values for potential at 50% activation of the normalized G–V curve ($V_{1/2}$) were −16.8 ± 1.5 mV 5 min after 1 μM TTX, −17.5 ± 1.2 mV 10 min after TTX and −16.9 ± 1.4 mV 15 min after TTX, and on the time-dependent effects, values for k did not show any statistical difference (Fig. 2d). These results indicate that F^- in the pipette solution had no significant effect on the background shift in the activation curve.

Concentration-dependent effects of PGE_2 on the TTX-R I_{Na}

To determine whether PGE_2 modifies TTX-R $I_{Na,}$ we examined concentration-dependent effects of PGE_2 on the current. A typical example of the effects of PGE_2 at different concentrations (0.01–10 μM) on the TTX-R I_{Na} evoked by depolarizing step pulses (−80 to

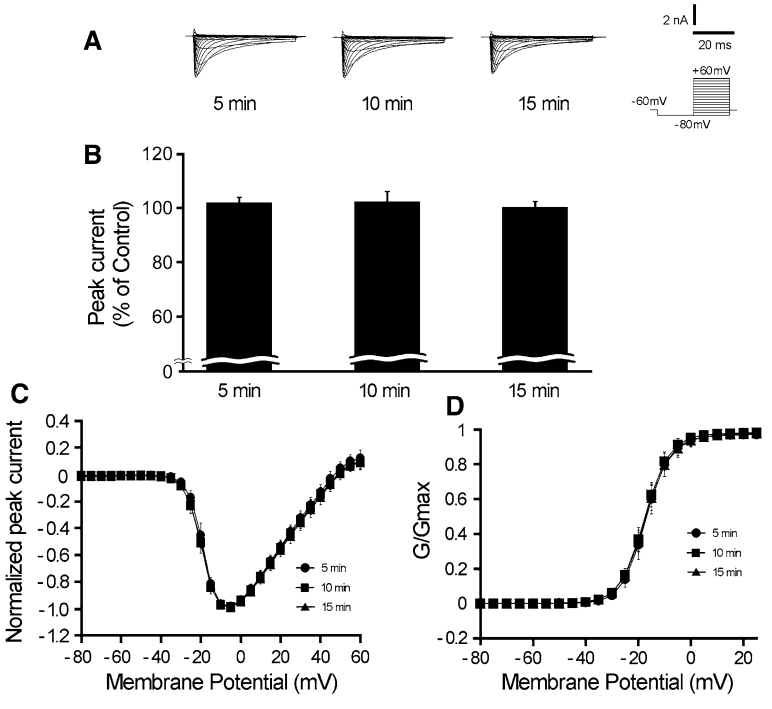

Fig. 2 Time-dependent effects of internal fluoride (F^-) on TTX-R Na^+ currents. **a** TTX-R Na^+ currents were obtained 5, 10 and 15 min after 1 μM TTX application. The cells were voltage-clamped at −80 mV and currents were recorded by stepping the potential between −80 and + 60 mV in 5 mV step duration (duration of each step, 50 ms). *Inset* voltage-pulse protocol. **b** Time-dependent effects of F^- on the percentage changes in the peak TTX-R I_{Na} amplitude. **c** Normalized current–voltage (I–V) curves were obtained 5, 10 and 15 min. Values show mean ± SEM ($n = 5$). **d** Normalized conductance–voltage (G–V) curves were obtained at 5, 10 and 15 min after 1 μM TTX application. Values show mean ± SEM ($n = 5$)

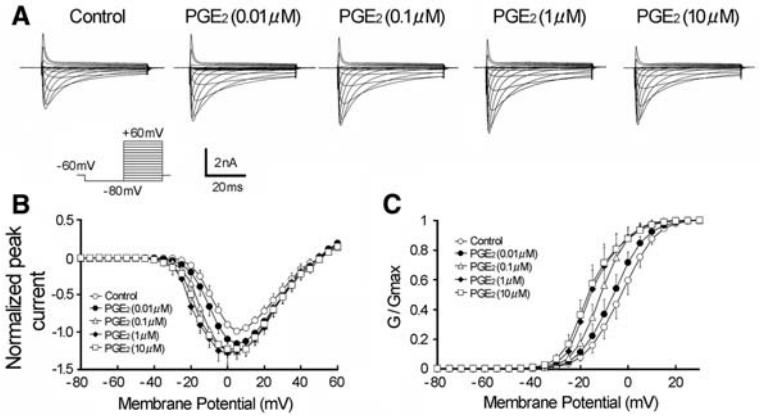

Fig. 3 Effects of PGE_2 applications on TTX-R Na^+ currents. **a** Typical TTX-R Na^+ current traces evoked by depolarizing step pulses before and after the application of PGE_2 at different concentrations (0.01, 0.1, 1 and 10 μM). The cell was voltage-clamped at −80 mV and the currents were recorded by depolarizing step pulses between −80 and + 60 mV in 5 mV steps (duration of each step, 50 ms). **b** Current–voltage (*I–V*) curves were obtained after PGE_2 application at 0.01, 0.1, 1 and 10 μM. Values show mean ± SEM ($n = 7$). **c** Normalized conductance–voltage (*G–V*) curves were obtained after the PGE_2 application at 0.01, 0.1, 1 and 10 μM. Values show mean ± SEM ($n = 7$). *$P < 0.05$, statistically significant difference from control values

+ 60 mV) is shown in Fig. 3a. Two minutes after PGE_2 applications ranging from 0.01 to 1 μM, it caused enhancement of peak TTX-R I_{Na} amplitude of the *I–V* curve in a concentration-dependent manner. The PGE_2 application up to 10 μM did not cause any significant difference on the peak TTX-R I_{Na} amplitude, as compared to that after 1 μM PGE_2 application. Figure 3b, c summarizes the effects of PGE_2 at different concentrations (0.01–10 μM) on TTX-R I_{Na} in seven cells.

The application of PGE_2 at 1 μM caused a maximal increase in the peak TTX-R I_{Na} (Fig. 3b, Table 2). The values for $V_{1/2}$ and k are summarized in Table 2. The $V_{1/2}$ potential obtained after 1 μM PGE_2 application was 8.3 mV more negative than that before the application. Concerning the values for k after PGE_2 applications (0.01–10 μM), there were no significant differences from control values.

Table 2 Effects of PGE_2 at different concentrations on the characteristics of TTX-R Na+ currents

	% Increase in the peak of *I–V* curve	$V_{1/2}$ for activation[a] (mV)	Slope factor (mV)
Control		−5.7 ± 1.2	5.5 ± 0.3
PGE_2 (0.01 μM)	17.0 ± 4.7*	−6.1 ± 2.4	5.4 ± 0.4
PGE_2 (0.1 μM)	26.8 ± 4.9*,**	−11.2 ± 2.2	4.6 ± 0.5
PGE_2 (1 μM)	31.1 ± 4.8*,**	−14.0 ± 2.3*,**	4.4 ± 0.3
PGE_2 (10 μM)	27.5 ± 3.4*,**	−14.3 ± 2.3*,**,#	4.5 ± 0.5

Values show mean ± SEM ($n = 7$)

*Statistical significant from control values ($P < 0.05$). **Statistical significant from 0.01 μM PGE_2 effects ($P < 0.05$). # Statistical significant from 0.1 μM PGE_2 effects ($P < 0.05$)

[a] Voltage on the activation for half of maximum current

Effects of PGE_2 on neuronal firing evoked by a depolarizing pulse

In the current-clamp mode, we tested how PGE_2 (1 μM) application modulates the activity of TTX-R TRG neurons. All tested cells were TTX-resistant. As shown in Fig. 4, the firing frequencies of action potentials after 1 μM PGE_2 application were increased when the magnitudes (1-3T) of depolarizing step pulses were increased, as compared to those before the application. As shown in Table 3, both the mean number of spikes and the overshoot of action potentials significantly increased after PGE_2 (1 μM) application. No significant differences in the resting membrane potential were found before and after 1 μM PGE_2 application (Table 3). Furthermore, there were no significant differences in the mean half duration of the first spike before and after 1 μM PGE_2 application (Table 3).

Discussion

The present study provided evidence that PGE_2 potentiated the excitability of small diameter TRG neurons retrogradely labeled with FG, which injected the superficial layer of the cervical dorsal horn, and this potentiation was mediated by an increase in the peak TTX-R I_{Na} amplitude accompanied by a hyperpolarizing shift in the activation curve. These results led us to

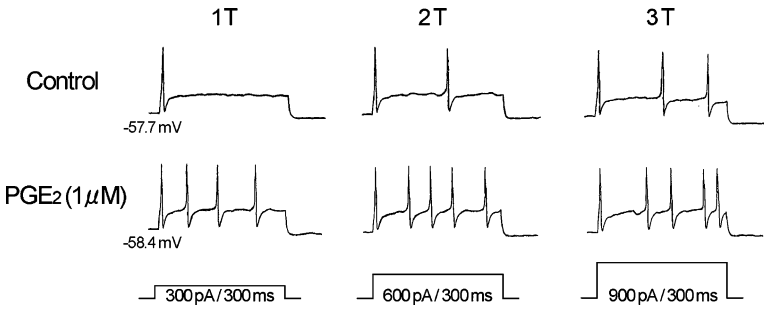

Fig. 4 Effects of PGE_2 on the neuronal firing evoked by depolarizing pulses. The action potential was induced at the threshold (T), two-times (2T) and three-times (3T) the threshold level, and these action potentials were resistant to TTX (1 μM). Application of PGE_2 (1 μM) increased the firing rates during depolarizing pulses, but had no significant effect on the resting membrane potentials

Table 3 Effects of PGE_2(1 μM) at different intensities on the number of action potentials

The magnitude of stimulation	Test agent	Number of spikes	Overshoot (mV)	Resting membrane potential (mV)	Duration at half-amplitude (ms)
1 Thereshold (T)	Control	1.2 ± 0.2	50.1 ± 1.9	−58.6 ± 1.2	−5.4 ± 0.9
	PGE_2 (1 M)	3.0 ± 0.4*	53.7 ± 1.5*	−55.6 ± 1.4	−4.8 ± 0.6
2 T	Control	2.0 ± 0.3#	51.3 ± 2.8	−59.2 ± 1.3	−5.5 ± 0.9
	PGE_2 (1 M)	4.0 ± 0.8*,**	58.0 ± 1.5*	−55.1 ± 1.8	−5.3 ± 0.7
3 T	Control	3.0 ± 0.5#,##	53.4 ± 2.9	−59.2 ± 1.5	−5.5 ± 1.1
	PGE_2 (1 μM)	5.6 ± 0.6*,**,***	58.0 ± 2.0*	−55.0 ± 1.6	−5.8 ± 0.9

Values show mean ± SEM ($n = 5$)

*Statistical significant from control values ($P < 0.05$). **Statistical significant from PGE_2 effects at 1T ($P < 0.05$). ***Statistical significant from PGE_2 effects at 2T ($P < 0.05$)

#Statistical significant from control values at 1T ($P < 0.05$). ## Statistical significant from control values at 2T ($P < 0.05$)

suggest that PGE_2 plays an important role in mediating the sensitization of TTX-R TRG neurons.

Appropriateness of the retrograde-labeling method

In this study, we used a retrograde tracer for the identification of the TRG neurons projecting onto the superficial C_1 region, as described in a previous study (Takeda et al. 2004). This technique has the advantage of determining their neuronal functions as compared to those of FG-negative small TRG neurons. Furthermore, no significant differences in the peak TTX-R I_{Na} amplitude were found between labeled and unlabeled TRG neurons. When considering these results, taken together, it is most likely that FG does not affect TRG neuronal excitability. Concerning the FG injection site represented by the C_1 region, this area is considered to be an extension of the caudalis in the trigeminal spinal nucleus, which receives most of its afferent inputs from the trigeminal nerve (Pfaller and Arvidsson 1988; Matsumoto et al. 1999; Tanimoto et al. 2002; Nishikawa et al. 2004; Takeda et al. 2005). There is evidence that c-Fos expression in superficial layer neurons at C_1–C_2 segments was found by varieties (thermal, mechanical and noxious) of the stimulation applied to the regions innervated by the trigeminal nerve (Strassman and Vos 1993; Coimbra and Coimbra 1994; Takeda et al. 1999). Therefore, it is possible to speculate the idea that FG-labeled small TRG neurons are nociceptive Aδ/C-type neurons. This idea was further supported by the fact that most of FG-labeled TRG neurons were less than 30 μm in diameter.

Potentiation of TTX-R I_{Na} by PGE_2

Although most TRG neurons express both TTX-sensitive (TTX-S) and TTX-R Na^+ currents, we measured the Na^+ current in the continuing presence of 1 μM TTX, as suggested by Fagan et al. (2001) and Matsumoto et al. (2005). The TTX-R I_{Na} is expressed preferentially in a population of small DRG neurons comprising the capsaicin-sensitive Aδ- and C-sensory neurons (Pearce and Duchen 1994; Arbuckle and Dockerty 1995) as well as in the termination of primary afferent fibers

(Aδ and C-fibers) that respond to noxious chemical and mechanical stimuli and to noxious heat (Bevan and Szolcssanyi 1990).

Using a perforated patch clamp, perturbations of the intracellular milieu are maintained to be minimal and diffusible transduction components, for example, cAMP, ATP and GTP, are not dialyzed out the cell. This patch-clamp technique is able to last for a relatively longer duration (> 60 min) and to be permeable to monovalent cations such as Na^+, but not to anions and divalent cations (Kyrozis and Reickling 1995). As the value for series resistance of the perforated patch electrode was maintained to be relatively higher (14.7 ± 0.7 MΩ), it may involve some voltage errors. We obtained evidence that no significant changes in the series resistance were observed throughout the experiments, as reported by Kwong and Lee (2005) in capsaicin-sensitive vagal pulmonary sensory neurons. But we cannot completely rule out the possibility that changes in the $V_{1/2}$ and k values of the activation curve seen after PGE_2 application may be due to a loss of voltage control.

In the present study, PGE_2 applications (0.01–10 μM) concentration-dependently increased the peak TTX-R I_{Na} amplitude and PGE_2 at 1 μM caused a maximal increase in the peak current accompanied by an 8.3 mV hyperpolarization shift of the activation curve. Recently, two different types of TTX-R Na^+ channels have been identified in sensory neurons: Nav 1.8 (SNS, PN3) and Nav 1.9 (NaN, SNS2) (Akopian et al. 1996; Sangameswaran et al. 1996; Dib-Hajj et al. 1998; Tate et al. 1998). The threshold for activation of Nav1.9 currents is near −70 mV and they show ultra-slow recovery from inactivation (Cummins et al. 1999). We could not observe in any TTX-R TRG neurons, having characteristics of Nav 1.9, in this study. Thus, the TTX-R I_{Na} of this study may belong to the category of Nav1.8 (slow TTX-R I_{Na}).

It has been reported that Nav 1.8 contributes substantially to action potential electrogenesis in C-type DRG neurons. For this reason, most Nav 1.8 (+/+) neurons generate all-or-none action potentials, whereas most Nav 1.8(-/-) neurons produce smaller graded responses (Renganathan et al. 2001). In current-clamp mode, we found that PGE_2 (1 μM) application significantly increased the number of action potential during depolarizing step pulses but had no significant effect on the resting membrane potential.

It has been reported that PGE_2 effects are mediated by G-protein-coupled EP (EP_1–EP_4) receptors (Narumiya et al. 1999). The fact that the mouse TRG neurons express the mRNA for EP_1–EP_4 receptors indicates that four subtypes of receptors may have some physiological functions (Borgland et al. 2002). Since the present study was designed to focus the effect of PGE_2 on the excitability of TRG neurons, we did not examine the effects of EP_1–EP_4 receptor agonists on the neuronal excitability.

Recently, Bar et al. (2004) reported that the application of PGE_2 agonists for EP_1, EP_2 and EP_4 receptors facilitated the response of dorsal horn neurons to mechanical stimulation of a normal knee, but that the EP_3 receptor agonist had no significant effect when the knee joint was normal. Matsumoto et al. (2005) also demonstrated that in neonatal nodose ganglion (NG) neurons, an increase in TTX-R I_{Na} induced by PGE_2 application was mediated by the activation of both EP_2 and EP_4 receptors. Thus, it is more likely that in TTX-R TRG neurons, potentiation of TTX-R I_{Na} seen after the PGE_2 application may involve an activation of both EP_2 and EP_4 receptors.

Increase in action potentials by PGE_2

In TTX-R TRG neurons retrogradelly labeled with FG, PGE_2 shifted the activation curve of TTX-R I_{Na} to more negative and enhanced the amplitude of the current. The results led us to suggest that these changes play important roles in determining the excitability of TTX-R TRG neurons. Electrophysiological properties of TTX-R I_{Na} currents in this study resemble those of the TTX-R I_{Na} acutely isolated neonatal rat NG neurons (Matsumoto et al. 2005). There is a tendency to show a decrease in the PGE_2-induced modulation of total voltage-dependent K^+ currents (England et al. 1996). Nevertheless, it has been reported that after application of 4-AP to inhibit I_A, the RMP is depolarized and the number of action potentials is increased in TRG neurons (Puil et al. 1989). Recently, we reported that TMJ inflammation increased the excitability of TRG neurons, innervating the region of TMJ, by suppressing I_A, but not I_K (Takeda et al. 2006). Thus, it is possible that I_A is linked to the firing rate and amplitude of action potentials. In the study using adult rat TTX-R TRG neurons, a slow inactivating transient current (I_D) contributes to the modification of neuronal function via inhibition of both I_A and I_K and the responses are not associated with any significant change in the RMP (Yoshida and Matsumoto 2005). Furthermore, they also found that after the functional loss of I_D due to α-dendrotoxin (α-DTX, 0.1μM) appliction, 50% inhibition of I_A or I_K still regulates firing properties of the action potential number and timing (Yoshida and Matsumoto 2005). Although there was the fact that the PGE_2 application had no significant effect on the RMP, further studies are needed to

elucidate the effects of PGE_2 on the relationships among three distinct different K^+ currents I_A, I_K and I_D as well as on the possible interactions between action potentials and these three K^+ currents.

References

Akopian AN, Sivilotti L, Wood JN (1996) A tetrodotoxin-resistant voltage-gated sodium channel expressed by sensory neurons. Nature 379:257–262

Arbuckle JB, Docherty RD (1995) Expression of tetrodotoxin-resistant sodium channels in capsaicin-sensitive dorsal root ganglion neurons of adult rats. Neurosci Lett 185:70–73

Arvidsson J, Raappana P (1989) An HRP study central projections from primary sensory neurons innervating the rat masetter muscle. Brain Res 480:111–118

Bar KJ, Natura G, Telleria-Diaz A, Teschner P, Vogel R, Vasquez E, Schaible HG, Ebersberger A (2004) Changes in the effect of spinal prostaglandin E_2 during inflammation:prostaglandin E (EP_1-EP_4) receptors in spinal nociceptive processing of input from the normal or inflamed knee joint. J Neurosci 24:642–651

Bereiter DA, Hirata H, Hu JW (2000) Trigeminal subnucleus caudalis: beyond homologies with the spinal dorsal horn. Pain 88:221–224

Bevan S, Szolcssanyi J (1990) Sensory neuron-specific actions of capsaicin: mechanisms and applications. Trends Pharmacol Sci 11:330–333

Borgland SL, Connor M, Ryan RM, Ball HJ, Christie MJ (2002) Prostaglandin E_2 inhibits calcium current in two sub-populations of acutely isolated mouse trigeminal sensory neurons. J Physiol (Lond) 539:433–444

Coimbra F, Coimbra A (1994) Dental noxious input reaches the subnucleus caudalis of the trigeminal complex in the rat, as shown by c-fos expression upon thermal or mechanical stimulation. Neurosci Lett 173:201–204

Cummins TR, Dib-Haji SD, Black JA, Akopian AN, Wood JN, Waxman SG (1999) A novel persistent tetrodotoxin resistant current in SNS-null wild type small primary sensory neurons. J Neruosci 19(RC439):1–6

Dallel R, Raboisson P, Auroy P, Woda A (1988) The rostral part of the trigeminal sensory complex is involved in orofacial nociception. Brain Res 448:1–19

Dib-Hajj SD, Black JA, Cummins TR, Kenney AM, Kocsis JD, Waxman SG (1998) Rescue of alpha-SNS sodium channel expression in small dorsal root ganglion neurons after axotomy by nerve growth factor in vivo. J Neurophysiol 79:2668–2676

Dray A (1995) Inflammatory mediators of pain. Br J Anaesth 75:125–131

England S, Bevan S, Docherty RJ (1996) PGE_2 modulates the tetrodotoxin-resistant sodium current in neonatal rat dorsal root ganglion neurones via the cyclic AMP-protein kinase A cascade. J Physiol (Lond) 495:429–440

Fagan KA, Schaack J, Zweifach A, Cooper DM (2001) Adenovirus encoded cyclic nucleotide-gated channels: a new methodology for monitoring cAMP in living cells. FEBS Lett 500:85–90

Gold MS (1999) Tetrodotoxin-resistant Na^+ currents and inflammatory hyperalgesia. Proc Natl Acad Sci USA 96:7645–7649

Gold MS, Levine JD, Correa AM (1998) Modulation of TTX-R I_{Na} by PKC and PKA and theier role in PGE_2-induced sensitization of rat sensory neurons in vitro. J Neurosci 18:10345–10355

Hu HZ, Li ZW (1996) Substance P potentiates ATP-activated currents in rat primary sensory neurons. Brain Res 739:163–168

Kwong K, Lee L-Y (2005) Prostaglandin E2 potentiates a TTX-resistant sodium current in rat capsaicin-sensitive vagal pulmonary sensory neurons. J.Physiol 564:437–450

Kyrozis A, Reichling DB (1995) Perforated-patch recording with gramicidin avoids artifactual changes in intracellular chloride concentration. J Neurosci Methods 57:27–35

Light AR, Perl ER (1979) Reexanimation of dorsal root projection to the spinal dorsal horn including observations on the differential terminataion of course and fine fibers. J Com Neuol 186:117–131

Marfurt CF, Turner DF U (1984) The central projections of tooth pulp afferent neurons in the rat as determined by the transganglionic transport of horseradish peroxidase. J Comp Neurol 223:535–547

Matsumoto S, Takeda M, Tanimoto T (1999) Effects of electrical stimulation of the tooth pulp and phrenic nerve fibers on C_1 spinal neurons in the rat. Exp Brain Res 126:351–358

Matsumoto S, Ikeda M, Yoshida S, Tanimoto T, Takeda M, Nasu M (2005) Prostaglandin E_2-induced modification of tetrodotoxin-resistant Na^+ currents involves activation of both EP_2 and EP_4 receptor in neonatal rat nodose ganglion neurones. Br J Pharmacol 145:503–513

Narumiya S, Sugimoto Y, Ushikubi F (1999) Prostanoid receptors structures: properties, and functions. Physiol Rev 79:1193–1226

Nishikawa T, Takeda M, Tanimoto T, Matsumoto S (2004) Convergence of nociceptive information from temporomandibular joint and tooth pulp afferents on C_1 spinal neurons in the rat. Life Sci 75:1465–1478

Pearce RJ, Duchen MR (1994) Differential expression of membrane currents in dissociated mouse primary sensory neurons. Neuroscience 63:1041–1056

Pfaller K, Arvidsson J (1988) Central distribution of trigeminal and upper cervical primary afferents in the rat studied by anterograde transport of horseradish peroxidase conjugated to wheat germ agglutinin. J Comp Neurol 268:91–108

Puil E, Miura RM, Spigelman I (1989) Consequences of 4-aminopyridine applications to trigeminal root ganglion neurons. J Neurophysiol 62:810–820

Rae J, Cooper K, Gates P, Watsky M (1991) Low access resistance perforated patch recordings using amphotericin B. J Neurosci Methods 37:15–26

Razook JC, Chandler MJ, Foreman RD (1995) Phrenic afferent input excites C1-C2 spinal neurons in rats. Pain 63:117–125

Renganathan M, Cummins TR, Waxman SG (2001) Contribution of Nav1.8 sodium channels to action potential electrogenesis in DRG neurons. J Neurophysiol 86:629–640

Sangameswaran L, Delgado SG, Fish LM, Koch BD, Jakeman LB, Stewart GR, Sze P, Hunter JC, Eglen RM, Herman RC (1996) Structure and function of a novel voltage-gated, tetrodotoxin-resistant sodium channel specific to sensory neurons. J Biol Chem 271:5953–5956

Sessle BJ (1987) The neurobiology of facial and dental pain: present knowledge, future directions. J Dent Res 66:962–981

Strassman AM, Vos BP (1993) Somatotopic and laminar organization of fos-like immunoreactivity in the medullary and upper cervical dorsal horn induced by noxious facial stimulation in the rat. J Comp Neurol 331:495–516

Sugiura Y, Lee CL, Perl ER (1986) Central projections of identified unmyelinated (C) affrent fubers innervating mammalian skin. Science 234:358–361

Takeda M, Tanimoto T, Ikeda M, Nishikawa T, Kawanishi N, Mohri M, Shimizu T, Matsumoto S (1999) Changes in c-Fos

expression induced by noxious stimulation in the trigeminal spinal nucleus caudalis and C1 spinal neurons of rats after hyperbaric exposure. Arch Histol Cytol 62:165–170

Takeda M, Tanimoto T, Ikeda M, Kadoi J, Nasu M, Matsumoto S (2004) Opioidergic modulation of excitability of rat trigeminal root ganglion neuron projections to the superficial layer of cervical dorsal horn. Neuroscience 125:995–1008

Takeda M, Tanimoto T, Ito M, Nasu M, Matsumoto S (2005) Role of capsaicin-sensitive primary afferent inputs from the masseter muscle in the C1 spinal neurons responding to tooth-pulp stimulation in rats. Exp Brain Res 160:107–117

Takeda M, Tanimoto T, Ikeda M, Nasu M, Kadoi J, Matsumoto S (2006) Enhanced excitability of rat trigeminal root ganglion neurons via decrease in the A-type potassium currents following temporomandibular inflammation. Neruoscience 138:621–630

Tanimoto T, Takeda M, Matsumoto S (2002) Suppressive effect of vagal afferents on cervical dorsal horn neurons responding to tooth pulp electrical stimulation in the rat. Exp Brain Res 145:468–479

Tate S, Benn S, Hick C, Trezise D, John V, Mannion RJ, Costigan M, Plumpton C, Grose D, Gladwell Z, Kendall G, Dale K, Bountra C, Woolf CJ (1998) Two sodium channels contribute to the TTX-R sodium current in primary sensory neurons. Nat Neuroscience 1:653–655

Yoshida S, Matsumoto S (2005) Effects of alpha-dendrotoxin on K^+ currents and action potentials in tetrodotoxin-resistant adult rat trigeminal ganglion neurons. J Pharmacol Exp Ther 314:437–445

Zimmermann M (1983) Ethical guidelines for investigations of experimental pain in conscious animals. Pain 16:109–110